Low Cost and Compact Active Integrated Antenna Transceiver for System Applications

Robert A. Flynt, Lu Fan, *Member, IEEE*, Julio A. Navarro, *Member, IEEE*, and Kai Chang, *Fellow, IEEE*

Abstract—**Integrated and active antennas incorporate component functions directly at the antenna terminals thereby reducing the size, weight, and cost of many microwave systems. Active integrated antennas have been used for distributed oscillators in spatial and quasi-optical power combining arrays, but the concept can be extended to include such applications as Doppler sensors, radars, and wireless communications to produce compact, low-cost products. In this paper, we report that a field-effect transistor (FET) and a Schottky mixer diode have been integrated within an inverted patch antenna for transceiver applications. The position of the mixer diode on the patch was optimized to achieve a minimum conversion loss. Preliminary results exhibit a 5.5 dB isotropic mixer conversion loss at 6 GHz for a 200 MHz intermediate frequency. The FET serves as both the transmitter and the local oscillator at 5.8 GHz. A two-way communication system using these transceivers is proposed.**

I. Introduction

INTEGRATED and active integrated antennas receive a great deal of attention because they can reduce the size, weight, and cost of many transmit and receive systems. Passive devices and active solid-state devices can be configured to provide several component functions at the terminals of the antenna. Active solid-state devices, for example, can be used to design active integrated antenna oscillators, amplifiers, and multipliers. These active integrated antennas are ideal for current investigations in spatial and quasi-optical power combining. The topic is intriguing since it involves several different areas of microwave engineering (i.e., solid-state devices, circuits, components, and antennas). Knowledge of circuit integration issues, component specifications, and material characteristics is also important.

Combination of guided-wave circuits with radiating structures in integrated antennas often leads to several performance trade-offs. Material properties that enhance circuit performance often degrade antenna radiation while dc biasing circuits and device packages disturb antenna characteristics. Similarly, an antenna's radiation may degrade a component's performance. Furthermore, component functions are connected directly to free space with little opportunity for nonquasi-optical processing or filtering. Overcoming these difficulties will allow integrated antennas to meet system requirements in military and commercial applications.

Since two- and three-terminal solid-state devices are small, lightweight, and easy to reproduce, they can be used to develop integrated antenna switches [1], tuners [2], detectors [3], mixers [4], amplifiers [5], oscillators [6], Doppler sensors [7], and receivers [8]. The choice between transistors and diodes depends on the type of microwave component required, operating frequency range, RF power output desired, available dc power input, as well as other considerations. The choice of solid-state device also affects the integrated antenna's radiation characteristics. In the past, active integrated antennas have deteriorated both the antenna and component performance. Unlike a passive antenna, an integrated antenna includes the effect of device packages and bias lines on the electromagnetic fields and surface currents. These effects often cause changes in operating frequencies, lower conversion efficiencies, and higher cross-polarization levels (CPL). If an integrated antenna can maintain reasonable component specifications with little degradation in the radiation characteristics, the approach would be attractive for many commercial and military systems.

This paper describes a transceiver made from the novel integration of a field-effect transistor (FET) and a mixer diode on the surface of an inverted patch antenna. The FET is configured within the inverted patch structure to oscillate at C-band. The oscillator acts as a transmitter, and couples a portion of its power to the mixer thereby also acting as a local oscillator. The optimal position for placing the mixer diode on the patch is determined. A Schottky diode is placed within the antenna cavity, and it receives a portion of the oscillator power that mixes with an incoming RF signal. For a 5.8 GHz LO and a 6 GHz incoming RF signal, the 200 MHz intermediate frequency exhibits 5.5 dB isotropic conversion loss (L_{iso}). This structure is different from those presented in [9]–[11] because the active devices are placed directly onto the patch that eliminates the need for interconnect lines. This structure is then incorporated into a two-way communication system.

II. Passive Inverted Patch Antenna

Fig. 1 shows the circular cavity backed inverted patch antenna that is used for the transceiver. The inverted patch configuration removes the ground plane from the substrate backside and inverts the conductor over a ground plane sup-

Manuscript received July 31, 1995; revised June 14, 1996. This work was supported in part by the U.S. Army Research Office and the Texas Higher Education Coordinating Board's Advanced Technology Program. J. A. Navarro is supported by a Training Grant from the NASA-Lewis Research Center in Cleveland, OH. The substrate material was provided by the Rogers Corporation.

R. A. Flynt was with the Department of Electrical Engineering, Texas A&M University, College Station, TX 77843-3128 USA. He is now with Texas Instruments Inc., Dallas, TX 75265 USA.

J. A. Navarro was with the Department of Electrical Engineering, Texas A&M University, College Station, TX 77843-3128 USA. He is now with the Epsilon Lambda Electronics Corp., Geneva, IL 60134 USA.

L. Fan and K. Chang are with the Department of Electrical Engineering, Texas A&M University, College Station, TX 77843-3128 USA.

Publisher Item Identifier S 0018-9480(96)06900-1.

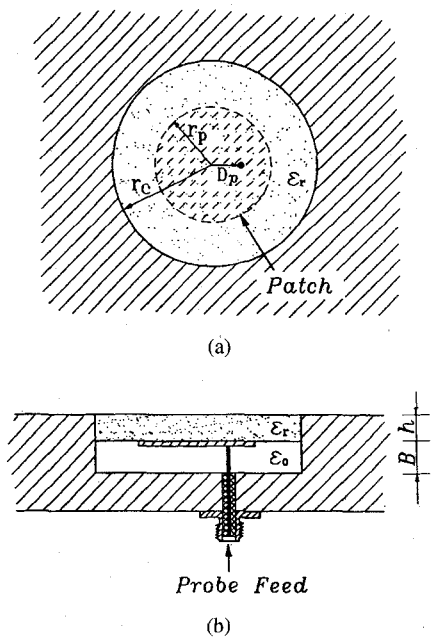

Fig. 1. Passive inverted stripline antenna backed by a circular cavity. (a) Top view showing the probe position. (b) Side view showing the probe and the cavity depth.

port. The electromagnetic fields are primarily concentrated in the air between the patch and the ground plane providing a lower effective dielectric constant (ε_{eff}), a longer guided wavelength, and higher characteristic impedance over a comparable line width in microstrip. The inverted patch uses a circular enclosure to isolate the antenna element and cut off possible surface modes that may be excited. The resulting trapped inverted microstrip geometry is a subset of the more general stripline-type transmission lines, hence the name [12], inverted stripline antenna.

The resonant frequency of an inverted circular patch antenna is calculated using a cavity model as in the microstrip patch and ignoring the bias modifications and integrated devices. The effective relative dielectric constant (ε_{eff}) and effective patch diameter (D_{eff}) are used to reconcile the differences with a conventional microstrip patch antenna cavity [13]

$$F_o = \frac{\alpha_{mn} c}{\pi D_{eff} \sqrt{\varepsilon_{eff}}} \tag{1}$$

where c is the speed of light and $\alpha_{mn} \approx 1.841$ for the dominant mode. D_{eff} is given by [14] shown in (2) shown at the bottom of the page where r_p is the physical patch radius, h is the substrate thickness and B is the patch-to-ground separation, as shown in Fig. 1. The structure's total height, $A = B + h$ is 4.5 mm. The diameters of the patch and cavity are 30 and 60 mm, respectively. The substrate used is RT-Duroid 5870 1.524 mm-thick with an $\varepsilon_r \approx 2.3$. Since the majority of the fields are concentrated within the air region (B), the ε_{eff} is near 1. An effective relative dielectric constant, $\varepsilon_{eff} \approx 1.1$ has previously shown less than 3% error for a wide range of frequencies and patch diameters [15]. A probe-fed, 30 mm diameter patch exhibited a VSWR of 1.0003 at 5 GHz and a 2 : 1 bandwidth of 3.77%. The E- and H-plane half-power beamwidths (HPBW's) are 57.5° and 61.5°, respectively. The cross-polarization level is 19.3 dB below the measured gain of 10.5 dBi.

III. Active Inverted Patch Antenna

Fig. 2 shows the active integrated antenna; the introduction of several dc blocks for biasing changes the performance dramatically with respect to the original circular patch. 0.1 mm wide gaps are etched to isolate the source, gate, and drain for dc biasing. Chip capacitors (82 pF) placed across the gap in the patch help to provide some RF continuity between the two halves of the patch. The capacitors are placed at 7.5 mm from the center of the patch in an area where the surface current is high on a passive circular patch antenna. DC biasing is achieved with voltage across the drain-to-gate (V_{DG}) and a 2 Ω chip resistor from the source to the gate. A similar FET integrated antenna [16] has previously demonstrated good oscillation and excellent radiation performance. In Fig. 2, the probe shown is used to measure the impedance at different points on the patch and the available LO power as will be discussed in Section IV.

The FET transistor used is an NEC-76 184AS. The bias (V_{DG}) is set between 3–5 V with a typical drain current of 40 mA. The oscillation frequency of the FET is a function of the cavity depth and the bias voltage. This allows for the signal to be modulated by applying a signal to the bias line. A bandwidth of 287 MHz was obtained by applying a 20 kHz signal to the drain bias line. This is about 5% modulation bandwidth for the carrier at 5.8 GHz.

IV. Transceiver Design

Fig. 3(a) and (b) show the complete integrated active antenna configuration. The equivalent circuit for the structure is shown in Fig. 3(c). Power from the oscillator is coupled to the mixer and is also transmitted from the antenna. The received power is coupled to the mixer in a similar manner. The IF power is taken from the bias lines and is passed through a low pass filter to remove the RF and LO signals.

The best possible position for placing the mixer diode on the patch should be one that offers good conversion loss, is physically realizable, and the active antenna radiating pattern should not adversely affected. All of these factors are strongly influenced by the position of the diode on the patch. To determine the optimal location for the mixer diode, several tests were conducted. The impedance of the mixer diode versus bias voltage and the impedance of the patch (seen by

$$D_{eff} = r_p \cdot \sqrt{1 + \left(\frac{2A}{\pi \cdot r_p \cdot \varepsilon_{eff}}\right)\left[\ln\left(\frac{r_p}{2A}\right) + 1.77 + 1.41\varepsilon_{eff} + \frac{A}{r_p}(0.268\varepsilon_{eff} + 1.65)\right]} \tag{2}$$

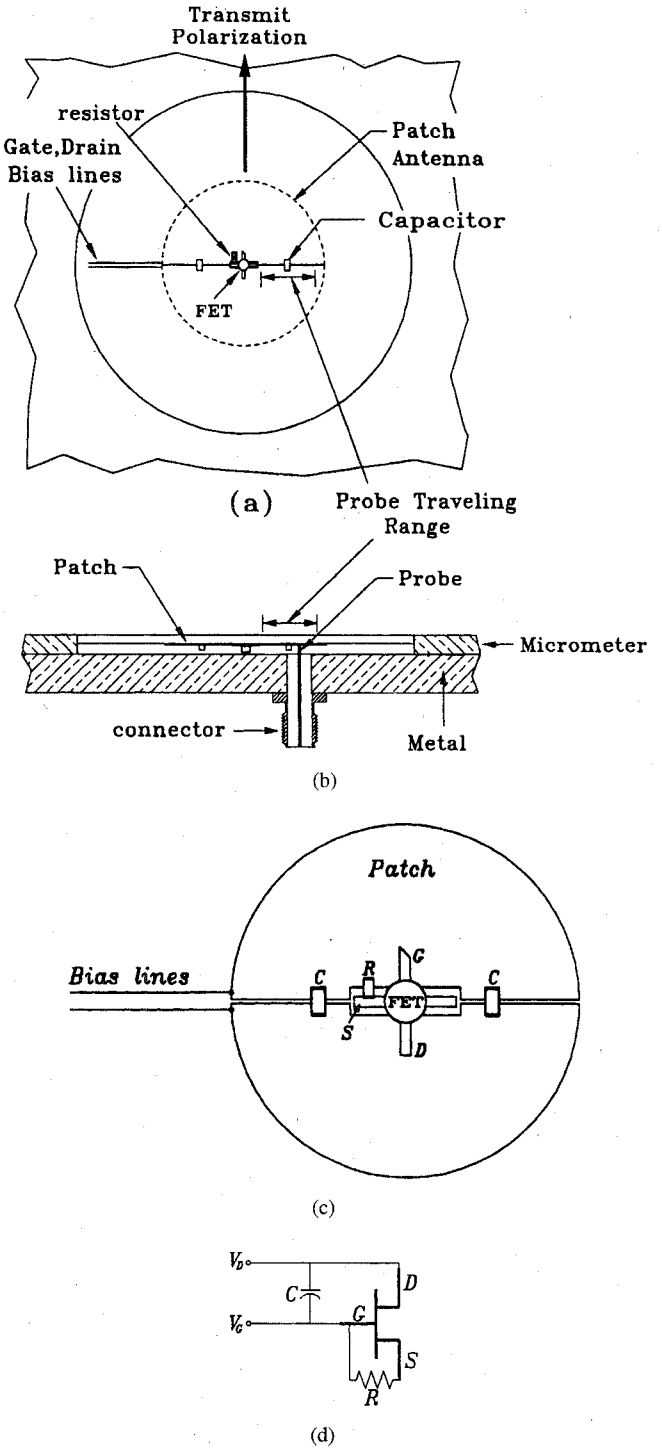

Fig. 2. Active inverted stripline antenna with a probe placed in the cavity for measurement purposes. (a) Top view showing the active devices and the capacitors placed across the gap. (b) Side view showing the probe and the probe traveling range. (c) Close-up view showing FET connections. (d) DC equivalent biasing circuit.

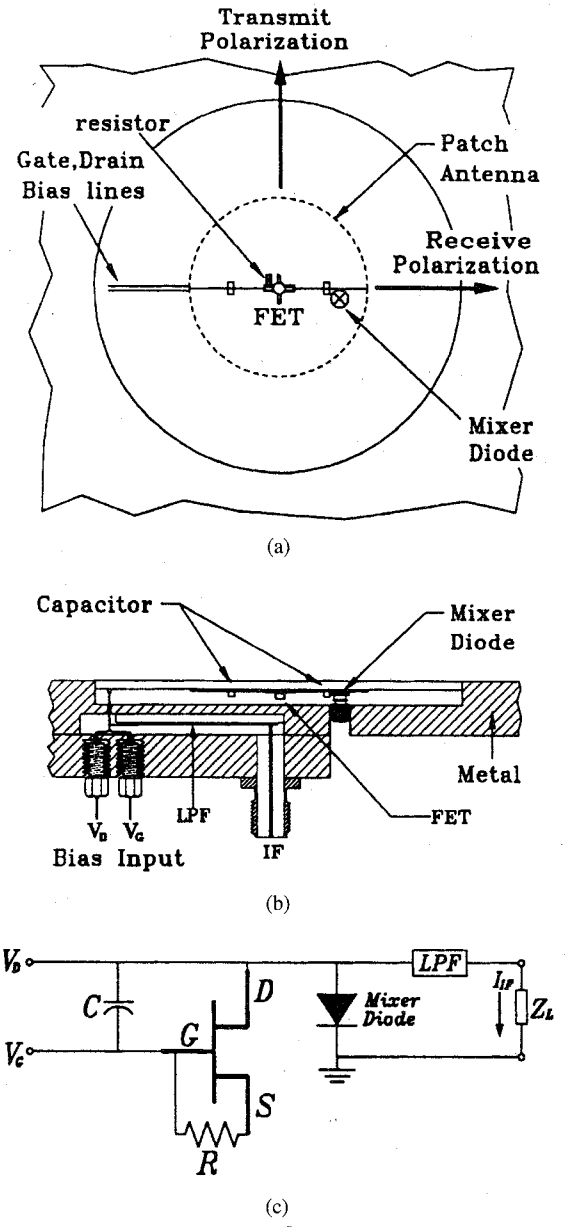

Fig. 3. Complete integrated active transceiver. (a) The top view showing the diode placement. (b) Side view showing the low pass filter. (c) Equivalent circuit for the integrated active antenna transceiver.

the diode) versus position were determined to try to achieve a reasonable impedance match between the diode and the patch. The available LO power was measured as a function of position as well as the available receive power versus position on the patch.

To conduct tests on the active patch antenna, a probe was placed into the cavity and was allowed to touch the patch as shown in Fig. 2. The probe is pressed onto the patch so that a good connection can be made. The probe can be used to measure the driving point impedance and available LO power at any position under the patch. The lower part of the cavity was constructed so that the cavity and the patch could be moved while the probe remained stationary. The position of the probe on the patch can be precisely controlled with a micrometer connected to the bottom of the cavity. This allows the impedance of the patch at various locations on the patch to be determined. The probe was connected to an HP 8510B Automatic Network Analyzer (ANA) and the resulting S-parameters were used to determine the input impedance at various points on the FET integrated active inverted patch antenna. The effect of the probe was modeled as an inductance. The value of the inductance was determined with the following

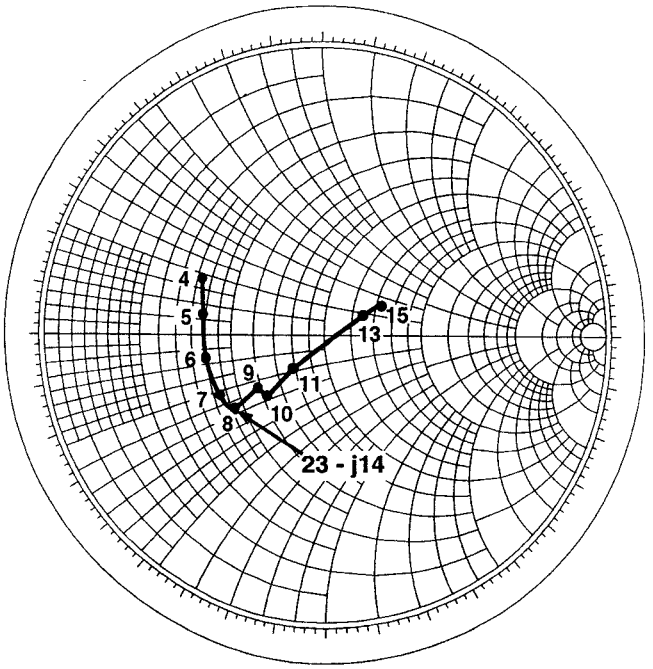

Fig. 4. Impedance versus position measured in mm for an active inverted patch antenna. The patch diameter is 30 mm. The positions shown are distances from the center of the patch to the probe.

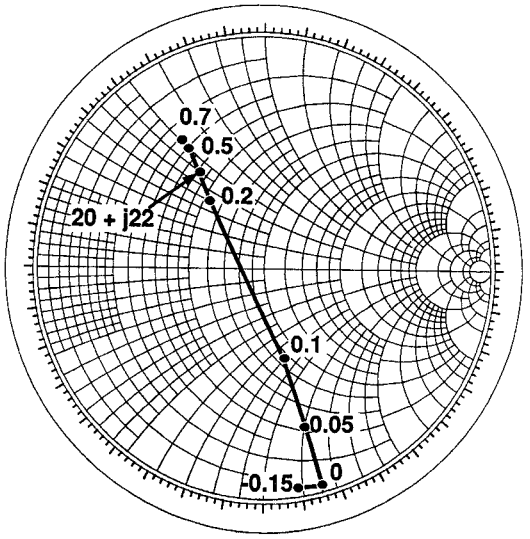

Fig. 5. Diode impedance versus bias voltage at 5.8 GHz. The numbers on the figure indicate bias voltage in volts.

expression [17]

$$X_L = \frac{120\pi l_p}{\lambda_o}\left[-0.5772 + \ln\left(\frac{2\lambda_o}{\pi d\sqrt{\varepsilon_r}}\right)\right] \qquad (3)$$

where l_p is the length of the probe and d is the diameter of the probe. The connector that was connected to the probe was modeled as a length of coaxial cable. The effects of the probe and the connector were de-embedded from the measured results to obtain the impedance of the patch seen by the diode. A plot of the patch impedance versus position is shown in Fig. 4 for 5.8 GHz. The results presented in Fig. 4 were obtained by moving the probe along a path that is parallel

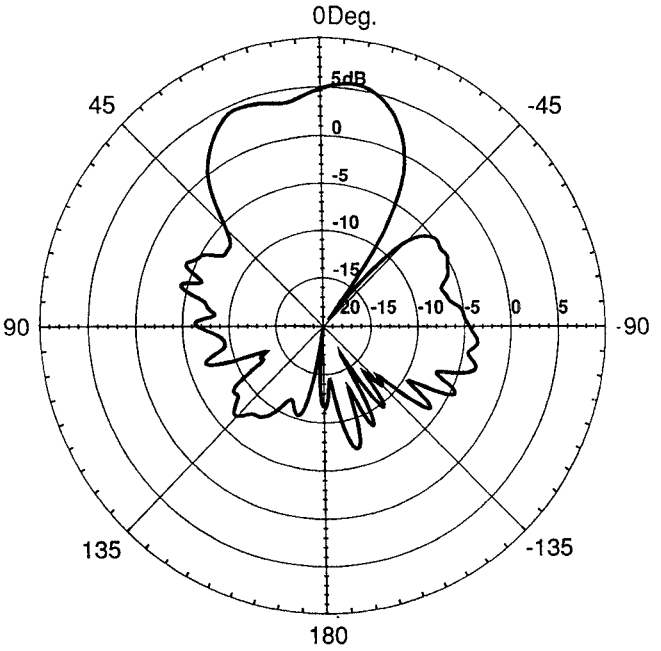

Fig. 6. The E-Plane receive pattern for the active integrated antenna. The pattern was measured with a probe placed at the final position for the mixer diode.

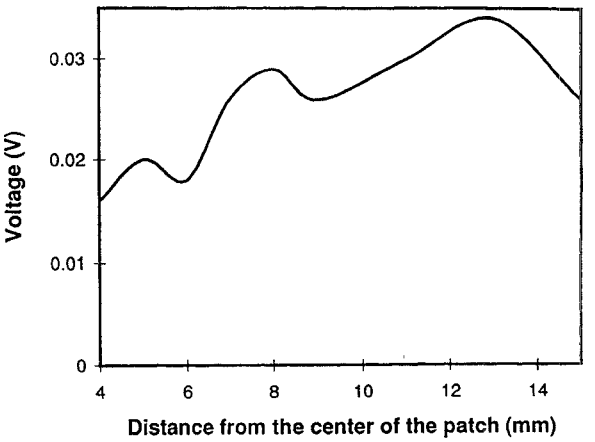

Fig. 7. Rectified dc voltage versus distance from the center of the patch measured in mm.

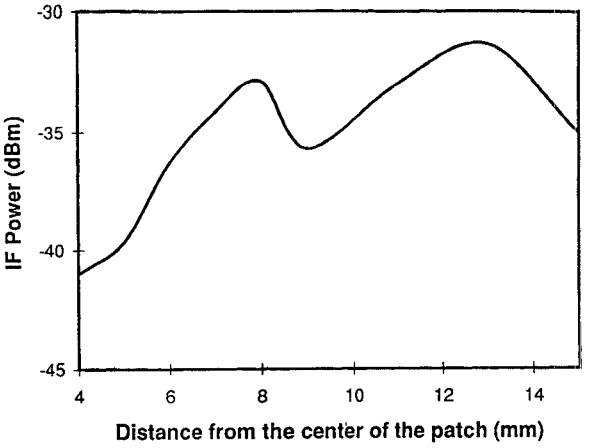

Fig. 8. Measured IF power versus distance from the center of the patch measured in mm.

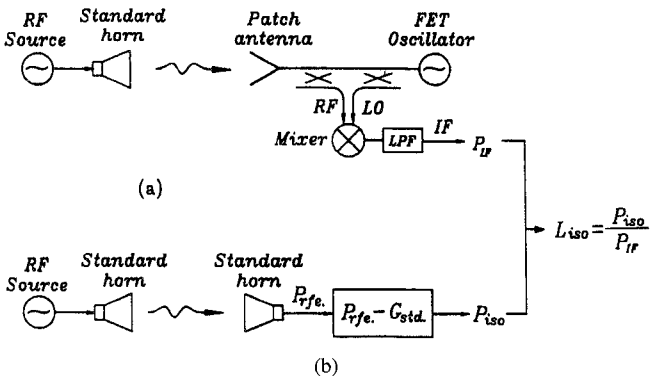

Fig. 9. Equipment set-up used to test the integrated antenna transceiver. (a) Test. (b) Reference.

to the bias cut. These measurements were obtained by using a network analyzer connected to the probe. The impedance measurements were conducted with the FET on (oscillating or large-signal) and with the FET off (not oscillating or small-signal). There is little change between the measurements for the frequency range of interest indicating little change in impedance with the FET on and off. The loading effects of the probe were determined by measuring the transmit pattern of the active antenna with the probe placed in the cavity. When the probe is placed along a path that is parallel to the bias cut the patterns are not adversely affected. The power from the measurement system is much smaller than the power from the FET oscillator so that measured results are accurate enough for the design. A second method was used for determining the impedance of the patch for areas where the power levels are too high for the network analyzer to handle. A stub tuner is connected to the probe and a spectrum analyzer is connected to the stub tuner. The stub tuner is adjusted until the power measured at the operating frequency is a maximum, indicating an impedance match to a 50 Ω load. The stub tuner is removed, and the spectrum analyzer is replaced with a 50 Ω load. The impedance looking into the stub tuner can then be measured with a network analyzer. This method produces reasonable results only near the operating frequency of the FET due to the narrow bandwidth of the stub tuner. This method is also limited by the resolution of the spectrum analyzer. These two methods for determining the patch impedance become less accurate in areas of the patch where the loading effects of the probe are more pronounced. In these areas there is a noticeable difference between the impedance measurements when the FET is on and when the FET is off.

The same probe configuration was used to determine the available LO power at different positions on the patch. The probe was connected to an adjustable tuning stub to match the probe to the 50 Ω measurement system. The available LO power is a maximum near the center and a minimum near the position of the capacitors. However, it was determined that there is sufficient LO power to pump the mixer diode for any physically realizable position on the patch because a low barrier diode was used.

The Schottky mixer diode used is a MA40191, and its I–V characteristics were measured using an HP-4145B curve tracer. A TRL calibration on an HP-8510B ANA was set up to

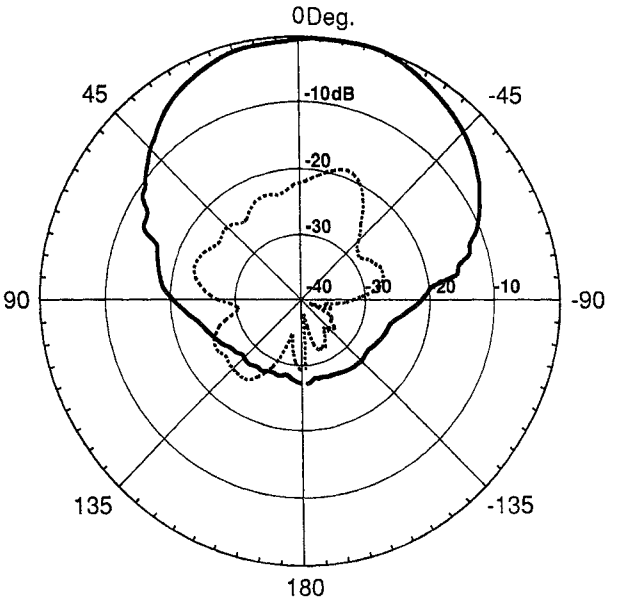

Fig. 10. H-plane pattern for the integrated antenna transceiver. The cross polarization level = − 18.8 dB and HPBW = 67° Solid line· copolarization, dashed line: cross-polarization.

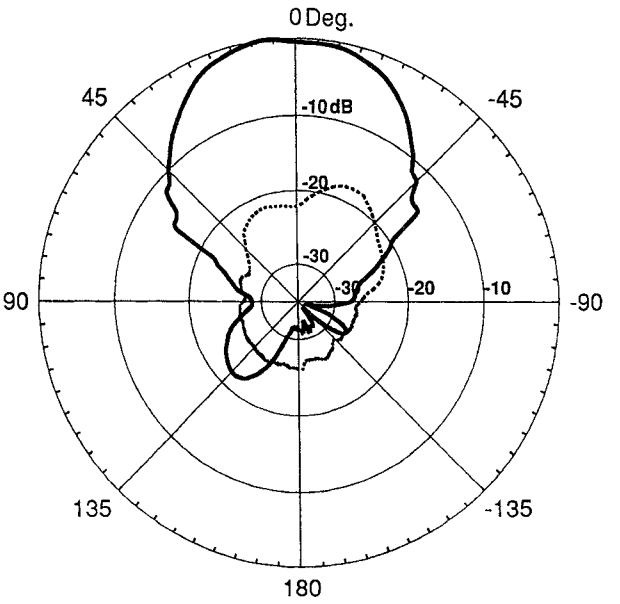

Fig. 11. E-Plane pattern for the integrated antenna transceiver. The cross polarization level = −17.99 dB and the HPBW = 49.3°. Solid line: copolarization, dashed line: cross-polarization.

characterize the diode impedance over the operating frequency range. The bias dependent data was used to curve-fit values to a standard diode model. The model was used to predict the impedance of the diode over a wide range of frequencies for various bias voltages. The impedance of the diode plotted as a function of bias voltage at 5.8 GHz is shown in Fig. 5. The impedance of the diode for zero and negative bias voltages is capacitive.

The receive pattern was measured by placing the active antenna into an anechoic chamber and taking the receive power from the probe. Fig. 6 shows the E-Plane receive

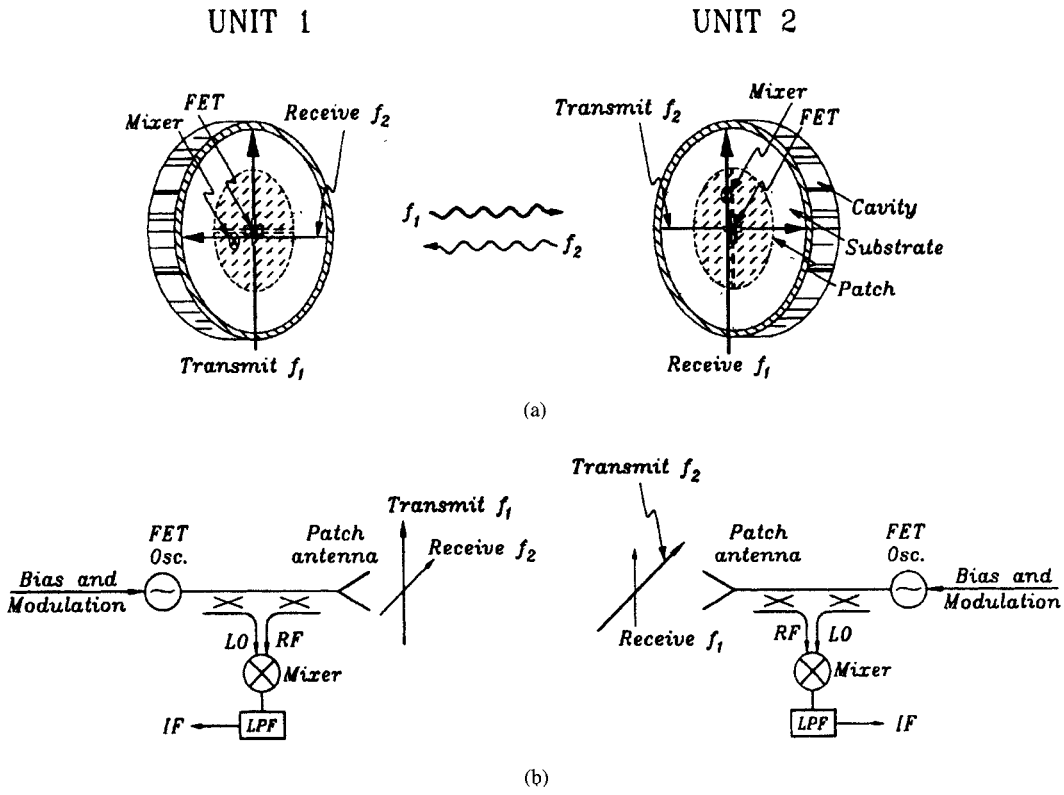

Fig. 12. Two-way radio using active antennas: (a) configurations and (b) block diagram.

pattern measured at the final position for the diode. These patterns were measured with the FET turned on. The resulting antenna gain was found to be about 6 dB at 5.75 GHz. This is somewhat lower than the value reported in [16], because the depth of the cavity had to be decreased due to the physical considerations of mounting the mixer diode. The addition of the active device may also have contributed to the change in performance. The null at $-45°$ in the pattern of Fig. 6 is possibly a result of the combined effects of the bias cut, bias lines, and the chip capacitors. The E-plane polarization is parallel to the bias cut, which could disturb the pattern.

The probe was removed from the back of the cavity and a mixer diode was placed into a fixture that replaces the probe. The mixer diode can be moved to different locations on the patch. A portion of the oscillator power will be rectified by the mixer diode. This results in a dc voltage across the diode. This also happens when an external signal is transmitted to the structure with the FET turned off. The external signal is obtained by connecting an RF source to a horn antenna and placing it 1 m away from the integrated active antenna transceiver. The rectified received voltage as a function of position can be used to approximate the relative received power as a function of position. The rectified dc voltage plotted as a function of position is shown in Fig. 7. The rectified dc voltage is a minimum near the center of the patch and is a maximum 13 mm from the center of the patch.

The best possible position for the mixer diode was determined using this information as well as ensuring that the active antenna radiation pattern was not adversely affected. The optimized position was determined to be 8 mm from the center of the patch on the gate side of the patch and very close to the bias cut, as shown in Fig. 3. This position was chosen because it provides a good compromise between the receive power, the impedance match, and the physical constraints of mounting the diode. The LO power is a minimum at this position, -12 dBm, but it is sufficient to pump the mixer diode. The rectified dc voltage due to the LO is 0.256 V when the diode is 8 mm from the center of the patch. This value is greater for any other position. At this position, the impedance of the patch is conjugate matched to the mixer diode as can be seen from Figs. 4 and 5 ($23 - j14$ at 8 mm in Fig. 4 and $20 + j22$ at 0.256 V in Fig. 5).

The IF power versus position is shown in Fig. 8. This measurement was made by applying an external RF signal to the patch and extracting the IF signal from the dc bias line via a low pass filter using thin wire. The external signal is obtained by connecting an RF source to a Narda 642 Standard Gain horn antenna and placing it 1 m away from the integrated active antenna transceiver. From Figs. 7 and 8, the IF power is a maximum near the same position that the rectified dc voltage is a maximum.

V. Circuit Performance

The active antenna is oriented to transmit vertical polarization while the mixer is positioned to receive horizontal polarization. Fig. 9 shows the equipment set-up used to test the integrated antenna transceiver. The transceiver showed an isotropic conversion loss of 5.5 dB with a 200 MHz IF. The

LO operated at 5.8 GHz, and the RF input was at 6 GHz. The mixer diode was removed and a probe was placed in its place so that the receive pattern for the inverted stripline antenna could be measured at the optimal position for the mixer diode. The value for the gain results in an approximate conversion loss for the mixer of 11.5 dB. The gain measurements can be used to determine the oscillator power output by placing a standard horn antenna as a receiver at a distance R away from the transceiver. The transmitting power is calculated by the Friis transmission equation [12]. The resulting output power was found to be 63 mW, resulting in a dc to RF conversion efficiency of 19%.

The transmit radiation patterns are similar to previous results in [16]. The half-power beamwidths and cross-polarization level (CPL) for the transmitter H-plane pattern are 67° and −18.8 dB, respectively. The half-power beamwidths and CPL for the transmitter E-plane pattern are 49.3° and 18 dB, respectively. Fig. 10 shows the H-plane pattern, and Fig. 11 shows the E-plane pattern.

VI. Two-Way Communication

The two-way communications system consisting of two integrated active patch antenna transceivers is proposed in Fig. 12. Each transceiver can be used to transmit and receive for simplex operation. The receive polarization is perpendicular to the transmit polarization for LO to RF isolation. One antenna can be rotated 90° with respect to the other, thus causing the transmit polarization for one transceiver to be equal to the receive polarization of the other transceiver. This allows for the polarization of a signal propagating in one direction to be perpendicular to a signal propagating in the opposite direction.

The maximum distance that the two transceivers can be separated was determined using the Friis transmission equation. The gain of the antenna is 6 dB. The minimum detectable signal (MDS) was determined by using the following expression [18]

$$\text{MDS} = 10 \log kT + 3 + 10 \log BW + F \qquad (4)$$

where k is the Boltzmann constant ($k = 1.38 \times 10^{-23}$ J/K), T is the absolute temperature in K, BW is the bandwidth in MHz, and F is the noise figure in dB for the system. Since this is not a self-oscillating mixer, the noise figure is estimated to be equal to the conversion loss [18]. The maximum range is calculated by

$$R_{\max}^2 = \frac{P_t G_t G_r}{\text{MDS}} \left(\frac{\lambda}{4\pi}\right)^2 \qquad (5)$$

where $R_{\max}$ is maximum range; P_t = 63 mW (transmit power); G_t = 6 dB (transmit antenna gain); G_r = 6 dB (receive antenna gain); λ = 0.05 m (wavelength at 6 GHz); MDS = −91.7 dBm. The maximum distance was estimated to be 4.8 km for a bandwidth of 6 MHz which is typical for a video signal.

VII. Conclusion

An integrated active antenna transceiver has been designed and successfully demonstrated. The active components were placed directly onto the patch antenna without compromising radiation performance. The circuit operates well with low conversion loss and low cross-polarization level. The circuit is well suited for commercial and military applications.

References

[1] J. A. Navarro and K. Chang, "Low-cost integrated inverted stripline antennas with solid-state devices for commercial applications," in *IEEE Int. Microwave Symp. Dig.*, 1994, pp. 1771–1774.

[2] P. Bhartia and I. J. Bahl, "Frequency agile microstrip antennas," *Microwave J.*, vol. 25, pp. 67–70, Oct. 1982.

[3] R. B. Waterhouse and N. V. Shuley, "Dual frequency microstrip rectangular patches," *Electr. Lett.*, vol. 28, no. 7, pp. 606–607, Mar. 26, 1992.

[4] K. D. Stephan and T. Itoh, "A planar quasi-optical subharmonically pumped mixer characterized by isotropic conversion loss," *IEEE Microwave Theory Tech.*, vol. MTT-32, no. 1, pp. 97–102, Jan. 1984.

[5] B. Robert, T. Razban, and A. Papiernik, "Compact amplifier integration in square patch antenna," *Electr. Lett.*, vol. 28, no. 14, pp. 1808–1810, Sept. 10, 1992.

[6] T. O. Perkins, "Active microstrip circular patch antenna," *Microwave J.*, pp. 109–117, Mar. 1987.

[7] V. F. Fusco, "Self-detection performance of active microstrip antennas," *Electr. Lett.*, vol. 28, no. 14, pp. 1362–1363, July 1992.

[8] U. Guttich, "Planar integrated 20 GHz receiver in slotline and coplanar waveguide technique," *Microwave Opt. Tech. Lett.*, vol. 2, no. 11, pp. 404–406, Nov. 1989.

[9] R. D. Martinez and R. C. Compton, "A quasi-optical oscillator/modulator for wireless transmission," in *IEEE MTT-S Int. Microwave Symp. Dig.*, 1994, pp. 839–842.

[10] K. Cha, S. Kawasaki, and T. Itoh, "Transponder using self-oscillating mixer and active antenna," in *IEEE MTT-S Int. Microwave Symp. Dig.*, 1994, pp. 425–428.

[11] D. Sanchez-Hernandez and I. Robertson, "60 GHz-band active microstrip patch antenna for future mobile systems applications," *Electr. Lett.*, vol. 30, no. 9, pp. 677–678, Apr. 28, 1994.

[12] J. A. Navarro, L. Fan, and K. Chang, "Active inverted stripline circular patch antennas for spatial power combining," *IEEE Trans. Microwave Theory Tech.*, vol. 41, no. 10, pp. 1856–1863, Oct. 1993.

[13] I. J. Bahl and P. Bhartia, *Microstrip Antennas.* Norwood, MA: Artech House, 1980.

[14] W. C. Chew and J. A. Kong, "Effect of fringing fields on the capacitance of a circular microstrip disk," *IEEE Trans. Microwave Theory Tech.*, vol. MTT-28, no. 2, pp. 98–104, Feb. 1980.

[15] J. A. Navarro, J. McSpadden, and K. Chang, "Experimental study of inverted microstrip for integrated antenna applications," in *IEEE Antennas Propagat. Int. Symp. Proc.*, Seattle, WA, 1994, pp. 920–923.

[16] J. A. Navarro, L. Fan, and K. Chang, "Novel quasi-optical active antenna using integrated FET inverted stripline patch," *Electr. Lett.*, no. 8, pp. 655–657, Apr. 14, 1994.

[17] B. Robert, T. Razban, and A. Papiernik, "Capacitors provide input matching of microstrip antennas," *Microwaves & RF*, pp. 103–106, Mar. 1987.

[18] K. Chang, *Microwave Solid-State Circuits and Applications.* New York: Wiley, 1994.

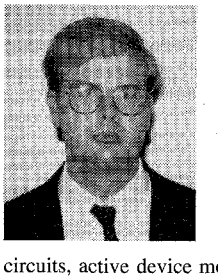

Robert A. Flynt was born in El Paso, TX, in 1969. He received the B.S. and M.S. degrees in electrical engineering from Texas A&M University, College Station, TX, in 1992 and 1995, respectively.

From 1994 to 1995, he worked to develop a compact active integrated antenna transceiver for system applications at Texas A&M University. Since October 1995, he has been a Design Engineer with Texas Instruments in Dallas, TX, where he is involved with nonlinear modeling of active devices His current interests are in microwave monolithic integrated circuits, active device modeling, and planar transmission line discontinuities.

Lu Fan (M'96) received the B.S. degree in electrical engineering from Nanjing Institute of Technology (current name Southeast University), Nanjing, China, in 1982.

From 1982 to 1990, he was with the Department of Radio Engineering of Nanjing Institute of Technology as a Teaching Assistant and Lecturer. In 1991, he became a Research Associate in the Department of Electrical Engineering, Texas A&M University, College Station, TX. His research interests include microwave and millimeter-wave components and active antennas.

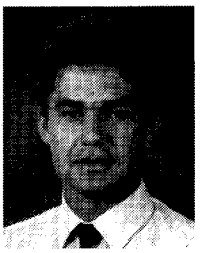

Julio A. Navarro (S'91–M'93) received the B.S., M.S., and Ph.D. degrees in electrical engineering from Texas A&M University, College Station, TX, in 1988, 1990, and 1995, respectively.

He was with General Dynamics, Fort Worth's cooperative education program from 1985 to 1991. At General Dynamics (now Lockheed-Fort Worth Company), he was a part of various groups including: Avionics Systems Design, Advanced Technology & Systems Engineering, Emitters & Intelligence, Antenna Systems, and Radar Cross-Section Research. He has designed wideband, low-observable antennas as well as many other printed circuit components. He was a Research and Teaching Assistant from 1989 to 1994. He has introduced many integrated and active integrated antennas such as Gunn-integrated varactor-tunable notch antennas. He has also integrated PIN, varactor, mixer, and Gunn diodes as well as transistors with inverted stripline patch antennas used for spatial power combining and beam steering applications. During this period, he developed novel Gunn VCO's, PIN switchable and varactor-tunable uniplanar filters, and ring resonators. In 1990, he was part of the group which designed and developed the Ka-band aperture-coupled circular patch antennas used in the NASA-Lewis *KaMIST* subarray project. He has published more than 20 technical papers and holds two patents in the microwave field. He has written a book (with Professor Kai Chang), *Integrated Active Antennas and Spatial Power Combining* (New York: Wiley, 1996). He and K. Chang are also co-authors of a chapter in an upcoming book, *Advances in Microstrip and Printed Antennas,* edited by K. F. Lee (to be published by John Wiley & Sons). Since 1994, he has been at Epsilon-Lambda Electronics Corporation where he designs and develops custom microstrip antenna arrays up to 94 GHz. He is currently working on cost-effective approaches for large, efficient phase scanned arrays using image line fed aperture-coupled microstrip patch antennas at Ka-band.

At Texas A&M University, Dr. Navarro received a Graduate Engineering Fellowship in 1989, a National Science Foundation Fellowship in 1991, the Ebensbarger Electrical Engineering Award in 1992, and a NASA-Lewis Research Center Training Grant in 1993.

Kai Chang (S'75–M'76–SM'85–F'91), for a photograph and biography, see this issue p. 1636.